Hao Wu
Key Laboratory of Advanced Reactor Engineering and Safety, Collaborative Innovation Center of Advanced Nuclear Energy Technology, Institute of Nuclear and New Energy Technology, Ministry of Education, Tsinghua University, Beijing 100084, China; School of Engineering, RMIT University, Melbourne 3083, VIC, Australia

Nan Gui
Key Laboratory of Advanced Reactor Engineering and Safety, Collaborative Innovation Center of Advanced Nuclear Energy Technology, Institute of Nuclear and New Energy Technology, Ministry of Education, Tsinghua University, Beijing 100084, China

Xingtuan Yang
Key Laboratory of Advanced Reactor Engineering and Safety, Collaborative Innovation Center of Advanced Nuclear Energy Technology, Institute of Nuclear and New Energy Technology, Ministry of Education, Tsinghua University, Beijing 100084, China

Jiyuan Tu
Key Laboratory of Advanced Reactor Engineering and Safety, Collaborative Innovation Center of Advanced Nuclear Energy Technology, Institute of Nuclear and New Energy Technology, Ministry of Education, Tsinghua University, Beijing 100084, China; School of Engineering, RMIT University, Melbourne 3083, VIC, Australia

Shengyao Jiang[1]
Key Laboratory of Advanced Reactor Engineering and Safety, Collaborative Innovation Center of Advanced Nuclear Energy Technology, Institute of Nuclear and New Energy Technology, Ministry of Education, Tsinghua University, Beijing 100084, China

Particle-Scale Investigation of Thermal Radiation in Nuclear Packed Pebble Beds

For the heat transfer of pebble or granular beds (e.g., high temperature gas-cooled reactors (HTGR)), the particle thermal radiation is an important part. Using the subcell radiation model (SCM), which is a generic theoretical approach to predict effective thermal conductivity (ETC) of particle radiation, particle-scale investigation of the nuclear packed pebble beds filled with monosized or multicomponent pebbles is performed here. When the radial porosity distribution is considered, the ETC of the particle radiation decreases significantly at near-wall region. It is shown that radiation exchange factor increases with the surface emissivity. The results of the SCM under different surface emissivity are in good agreement with the existing correlations. The discrete heat transfer model in particle scale is presented, which combines discrete element method (DEM) and particle radiation model, and is validated by the transient experimental results. Compared with the discrete simulation results of polydisperse beds, it is found that the SCM with the effective particle diameter can be used to analyze behavior of the radiation in polydisperse beds. [DOI: 10.1115/1.4039913]

Keywords: particle radiation, pebble bed, particle scale, radial porosity, emissivity, polydisperse bed

1 Introduction

Particle thermal radiation is an important process of heat transfer in high temperature gas-cooled reactors (HTGR), which is an advanced type nuclear reactor of inherent safety [1–3]. The reactor core is a dense packed pebble bed filled with many fuel spheres. The highest operation temperature of the pebbles is about 800 °C and it can reach 1600 °C under nuclear accidents.

In early stage of investigating the particle radiation in packed pebble beds, the most efforts focus on the experimental measurements and develop the related empirical correlations [4–6]. The particle radiation flux and the effective thermal conductivity (ETC) increase greatly under high temperatures in the packed

[1]Corresponding author.

Contributed by the Heat Transfer Division of ASME for publication in the Journal of Heat Transfer. Manuscript received November 15, 2017; final manuscript received April 2, 2018; published online May 22, 2018. Editor: Portonovo S. Ayyaswamy.

pebble beds [7–9]. Then, the correlations of ETC are extended to the polydisperse beds of multicomponent spheres [10,11]. In recent years, the experimental facilities targeted for HTGR, such as high temperature test unit (HTTU) [12] and test facility-pebble bed equivalent conductivity (TF-PBEC) [13,14], are tested, and the operation conditions are similar to those in the core of HTGR. When the solid conductivity of the particle material is close to the ETC of the particle radiation, the effect of the solid conductivity on the particle radiation is significant [15,16].

For the theoretical evaluation, two-flux radiation model [17] and ray tracing method [18] are reported. The pebble beds are modeled as the isotropic homogeneous medium of absorption, scattering and emitting. However, it is the scattering coefficient and absorption coefficient of the packed pebble beds rather than the physical properties of the pebbles, such as surface emissivity and solid conductivity applied in the numerical model. At low surface emissivity, two-flux radiation model and ray tracing method are no longer applicable [19].

Discrete element method (DEM) now is widely accepted in the simulations of the packing, pebble flow [20], and the mixing [21]. Similarly, the particle radiation in the packed pebble bed is very meaningful to be investigated in the particle scale. With the physically reasonable simplification, the particle-scale method called short-range radiation model (SRM) is developed in our previous work [16]. The SRM is efficient in the calculation and the numerical results are in good agreement with the experimental data [16]. With SRM in packed pebble beds, the framework of computational fluid dynamics (CFD)–DEM coupling with particle radiation is discussed and the simulations of HTR-10 benchmark are performed [22,23]. Moreover, when the particle temperature exceeds 1200 °C, the SRM will overestimate the radiation flux in the packed pebble beds [16,24]. Thus, under very high temperature ranges (over 1500 °C), subcell radiation model (SCM) proposed in Ref. [24] is recommended, in which the porosity, surface emissivity, and solid conductivity are taken into account.

In this work, particle-scale investigation of thermal radiation is performed for the nuclear packed pebble beds. The radial porosity distribution of the wall effect on the particle radiation and surface emissivity are discussed. The predicted values of SCM are compared with the experimental data and empirical correlations. Combined with SCM and the DEM, particle motion and transient heat transfer model is presented and applied in the analysis of the multicomponent polydisperse beds.

2 Particle-Scale Radiation Model

2.1 Subcell Radiation Model. In order to predict ETC of particle thermal radiation, SCM is developed in our previous work [24], which is a generic theoretical method. The subcell of the face centered cubic (FCC) packing for particle radiation is shown in Fig. 1. The Voronoi tessellation of the FCC packing is a rhombic dodecahedron for every particle. Point O_1 and point O_2 are the center positions of the particles, and surface *ABCD* is the subsurface of the Voronoi cell connected with the two particles. Based on the gray surface radiation theory and combined with the Schotte equation [15], ETC of thermal radiation ($k_{r,\mathrm{SCM}}$) is formulated as

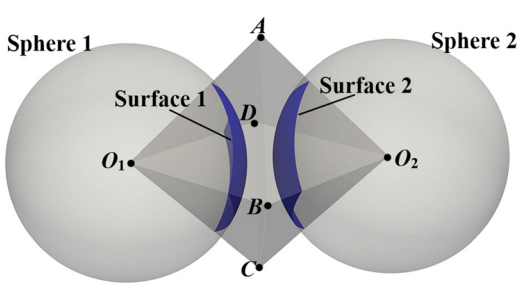

Fig. 1 Subcell of the FCC packing in particle radiation model

$$k_{r,\mathrm{SCM}} = \frac{1-\varepsilon}{\dfrac{1}{k_s}+\dfrac{1}{k_\infty}} + \varepsilon k_\infty \tag{1}$$

$$k_\infty = \frac{3}{2\Gamma\left(\dfrac{5}{3}\right)}\left(\frac{\sqrt{2}\pi}{6}\right)^{1/3}\frac{(1-\varepsilon)^{1/3}}{\varepsilon}\frac{\sigma d_p T^3}{\dfrac{1-\varepsilon_r}{\varepsilon_r}+\dfrac{1}{1+V_{12}}} \tag{2}$$

in which ε and ε_r are the porosity of the bed and emissivity of the particle surface, respectively; k_s is solid conductivity of the particle material; and k_∞ is the value of ETC when k_s is infinity. d_p and T are the diameter and temperature of the particle, respectively; σ is the Stefan–Boltzmann constant (5.670367×10^{-8} W m^{-2} K^{-4}); V_{12} is the view factor between surface 1 and surface 2, and it can be calculated by numerical integral under different porosity [24]; And $\Gamma(\bullet)$ is the gamma function, and it is defined as

$$\Gamma(x) = \int_0^{+\infty} u^{x-1}e^{-u}\mathrm{d}u \tag{3}$$

Random modification factor is considered in the SCM [24]. The particle in the Voronoi cell is smaller than the inscribed sphere of the rhombic dodecahedron. Thus, particle diameters are $d_p = \beta d_i$ and $0 < \beta \le 1$, in which d_i is the diameter of the inscribed sphere. The relationship between the porosity and the parameter β is expressed as

$$\varepsilon = 1 - \frac{\sqrt{2}}{6}\pi\beta^3 \tag{4}$$

With the scale factor β, the view factor V_{12} in SCM can be obtained under different porosity. From the numerical results, V_{12} is 0.3955 at $\varepsilon = 0.39$ (dense packing) and 0.3561 at $\varepsilon = 0.44$ (loose packing). Solid conductivity k_s under different temperatures in nuclear packed pebble beds is available from the experimental measurements [14,25].

2.2 Effect of Radial Porosity Distribution. In the previous discussion [24], only uniform porosity distribution is applied in the packed pebble bed. However, from the experimental data [12] and numerical simulations [26,27], it is shown that the capability of heat transfer in near-wall region is different from that in the bulk region. For the cylindrical beds, such as nuclear reactors [1–3] and the related experimental facilities [12,14,28], radial heat transfer equation is written as

$$Q(r) = -2\pi r L(k_c + k_{r,\mathrm{SCM}})\frac{\mathrm{d}T(r)}{\mathrm{d}r} \tag{5}$$

in which $Q(r)$ is the heat flux at the radial position r; L is the height of the bed; and k_c is the ETC of the conduction, and it can be calculated by empirical models or experimental data [19,29,30]. For the uniform porosity distribution, $k_{r,\mathrm{SCM}}$ is only determined by the temperature with the constant physical properties. In this case, Eq. (5) can be solved by an implicit analytical solution and the wall effect on the ETC is neglected [24].

Radial porosity distribution in the packed pebble bed is considered to investigate the wall effect and nondimensional distance to the physical walls in the cylindrical beds is defined as

$$\xi = \begin{cases} \dfrac{R_o - r}{d_p}, & r \le \dfrac{R_o + R_i}{2} \\ \dfrac{r - R_i}{d_p}, & r > \dfrac{R_o + R_i}{2} \end{cases} \tag{6}$$

in which R_i and R_o are the radii of the inner wall and the outer wall, respectively. Basically, porosity increases greatly near the

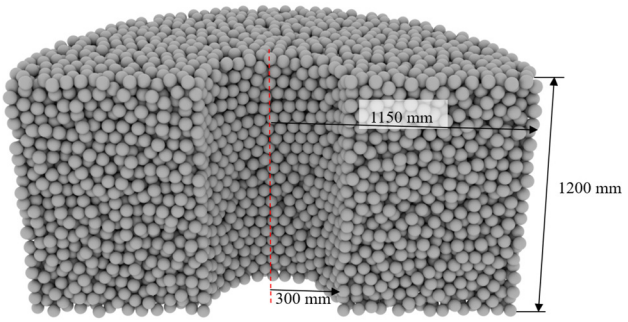

Fig. 2 The geometry and packing of HTTU experiment (sectional view)

wall and the radial porosity distribution in White model [31] is formulated as

$$\varepsilon(r) = \left[1 + \frac{1-\varepsilon_\infty}{\varepsilon_\infty}\sqrt{1-\exp(-2\xi)}\right]^{-1} \tag{7}$$

in which ε_∞ is the porosity in the bulk region, which is far away from the physical walls. In the discussion of the heat convection in packed beds [32,33], the porosity distribution is written in the exponential form

$$\varepsilon(r) = \varepsilon_\infty\left[1 + \frac{1-\varepsilon_\infty}{\varepsilon_\infty}\cdot\exp(-N\xi)\right] \tag{8}$$

in which N is the shape parameter, and it is discussed by many researchers [32,34,35]. The value recommended by Hunt and Tien [36] is $N = 6$. Alternatively, the damped oscillatory distribution of radial porosity is first reported by Benenati and Brosilow [37]. The Mueller model [38] is given as

$$\varepsilon(r) = \varepsilon_\infty + (1-\varepsilon_\infty)\exp(-a\xi)J_0(b\xi) \tag{9}$$

in which a and b are the shape parameters [19]. From the simulation results of DEM, area-based porosity distribution proposed by De Klerk [39] is formulated as

$$\varepsilon(r) = \begin{cases} 2.14\xi^2 - 2.35\xi + 1, & \xi \le 0.637 \\ \varepsilon_\infty + 0.29\exp(-0.6\xi)\cos(2.3\pi(\xi - 0.16)) & \\ +0.15\exp(-0.9\xi), & \xi > 0.637 \end{cases} \tag{10}$$

The packed pebble bed of HTTU experiment [12] is chosen to investigate the wall effect of particle radiation. The geometry and packing simulated by DEM are shown in Fig. 2. The radii of walls are $R_i = 300$ mm and $R_o = 1150$ mm. The height of the bed is 1200 mm, and it is filled with about 25,000 machined graphite pebbles of 60 mm in diameter. The inner wall is heated by heater elements with the net power of about 66.38 kW. The volume-based porosity [34,38,40] at radial position r is defined as

$$\varepsilon(r) = 1 - \frac{\sum_{i=1}^{n} V_{p,i}\Big|_{r-\Delta r}^{r+\Delta r}}{L\cdot\int_{r-\Delta r}^{r+\Delta r} 2\pi r\mathrm{d}r} \tag{11}$$

in which $V_{p,i}|_{r-\Delta r}^{r+\Delta r}$ is the volume of particle i segment in the radial distance $r-\Delta r \sim r+\Delta r$. In present particle scale discussion, integral length is the particle diameter or distance to the physical walls, i.e., $2\Delta r = \min(d_p, 2\xi d_p)$. When the integral length $2\Delta r$ tends to 0, it will be the area-based porosity [34].

The numerical results of the volume-based and area-based porosity are shown in Fig. 3. It is shown that the volume-based result of DEM is in good agreement with that of White model. The De Klerk model accords well with the area-based distribution. The radial porosity of White model, De Klerk model, and uniform distribution is applied to solve the radial heat equation separately. The constant surface emissivity ($\varepsilon_r = 0.8$), constant ETC of conduction ($k_c = 2\ \mathrm{W\,m^{-1}\,K^{-1}}$), and experimental solid conductivity [12,14] are applied in the simulations. Radial effective thermal conductivity ($k_{\mathrm{eff}} = k_c + k_{r,\mathrm{SCM}}$) is the function of the particle temperature and porosity at the radial position r. With the De Klerk model (see Fig. 4(*a*)), damped oscillatory ETC of particle radiation is emerged in near-wall region. But the experimental ETC decreases monotonically when it comes close to the physical walls. The results of the volume-based White model shown in Fig. 4(*b*) are in general agreement with the experimental data with wall effect. Because the SCM is a particle-scale approach, the volume-based porosity in particle scale is more appropriate to be applied in the heat transfer simulations.

2.3 Effect of Surface Emissivity. The surface emissivity is an important parameter in the particle radiation calculation and it is affected by many factors, such as optical properties, temperature [41], surface roughness [42], and the oxidation [43]. When the solid conductivity is far greater than the ETC of particle radiation ($k_s \gg k_r$) or operated in low temperature, the radiation exchange factor F is the single-valued function of the surface

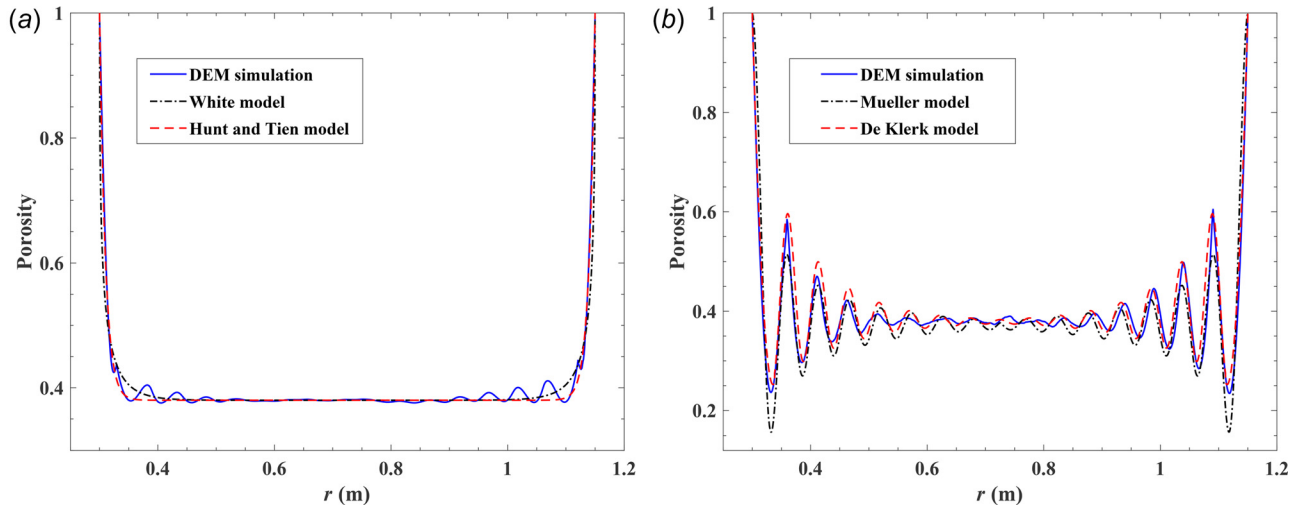

Fig. 3 Volume-based (*a*) and area-based (*b*) radial porosity distribution of the packed pebble bed

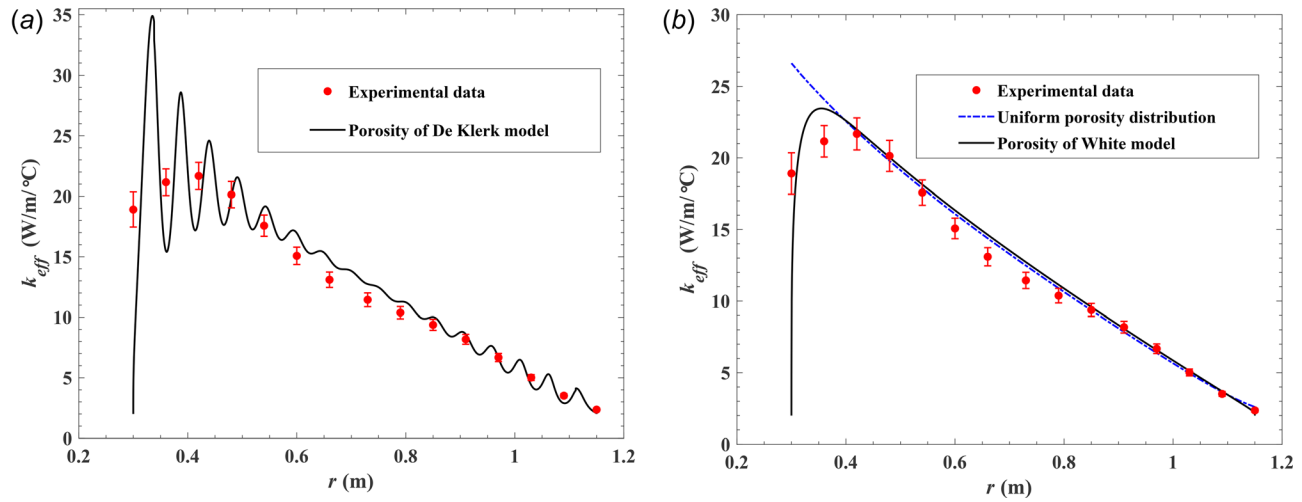

Fig. 4 Radial ETC with area-based (*a*) and volume-based (*b*) porosity distribution

emissivity for the packed pebble beds of dense packing, which is defined as

$$F = \frac{k_r}{4\sigma d_p T^3} \tag{12}$$

From the mechanism of the thermal radiation, the radiation exchange factor should fulfill the following conditions

$$\lim_{\varepsilon_r \to 0} F(\varepsilon_r) = 0 \tag{13}$$

$$\frac{\mathrm{d}F(\varepsilon_r)}{\mathrm{d}\varepsilon_r} > 0 \tag{14}$$

Based on the experimental measurement, Nasr model [9] is given as

$$F = \varepsilon_r \tag{15}$$

From the Argo model [44], the radiation exchange factor is written as

$$F = \frac{1}{2/\varepsilon_r - 1} \tag{16}$$

And in Wakao model [45], F is formulated as

$$F = \frac{2}{2/\varepsilon_r - 0.264} \tag{17}$$

The results of SCM and mentioned above model in nuclear packed pebble beds of dense packing ($\varepsilon = 0.39$) are shown in Fig. 5. For all concerned models, the radiation exchange factor increases with the surface emissivity and F tends to 0 when ε_r goes to 0. The SCM is in good agreement with the Nasr model and Wakao model, and it is slightly greater than the Argo model.

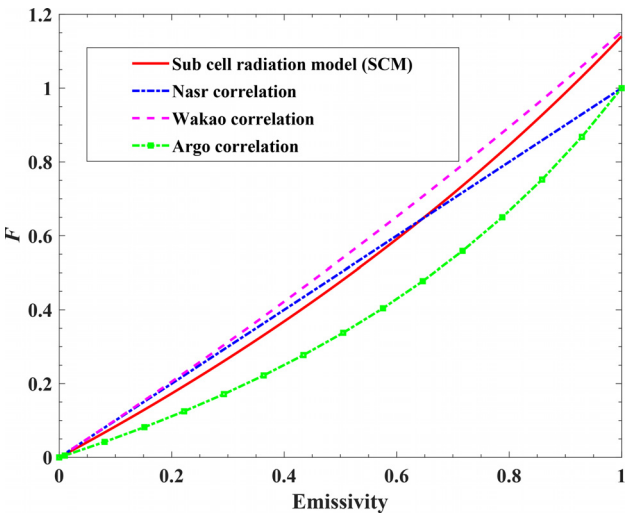

Fig. 5 Radiation exchange factor under different surface emissivity in dense packed pebble beds

3 Discrete Simulation

3.1 Particle-Scale Heat Transfer Model. Combined with the DEM, particle motion of elastic Hertz–Mindlin model [46,47] and the heat transfer equations at time t are written as

$$m_i \frac{\mathrm{d}\boldsymbol{u}_i}{\mathrm{d}t} = \sum_{j=1}^{n} (\boldsymbol{F}_{n,ij} + \boldsymbol{F}_{t,ij}) + m_i \boldsymbol{g} + \boldsymbol{F}_{f,i} \tag{18}$$

$$I_i \frac{\mathrm{d}\boldsymbol{\omega}_i}{\mathrm{d}t} = \boldsymbol{M}_r + \mathbf{R}_i \times \sum_{j=1}^{n} \boldsymbol{F}_{t,ij} \tag{19}$$

$$C_i m_i \frac{\mathrm{d}T_i}{\mathrm{d}t} = -k_{ij} \frac{A_{ij}}{L_{ij}} (T_i - T_j) + q_f + q_s \tag{20}$$

in which $\boldsymbol{u}_i$, $\boldsymbol{\omega}_i$, and T_i are the velocity, angular velocity, and temperature of the particle i, respectively; m_i, I_i, and C_i are the mass, moment of inertia and specific heat, respectively; $\boldsymbol{F}_{n,ij}$ and $\boldsymbol{F}_{t,ij}$ are the normal and tangential contact forces, respectively; $\boldsymbol{F}_{f,i}$ and $\boldsymbol{M}_r$ are the fluid–particle interaction force and rolling friction torque; R_i and $\boldsymbol{g}$ are the particle radius and the gravity, respectively; q_f and q_s are the heat convection term and the heat source, respectively. For the two Voronoi neighboring particles (see Fig. 6), A_{ij} is the area of the Voronoi face and L_{ij} is the distance between the particle centers. k_{ij} is the equivalent conductivity including conduction and particle radiation, which is calculated by

$$\frac{l_i + l_j}{k_{ij}} = \frac{l_i}{k_i} + \frac{l_j}{k_j} \tag{21}$$

$$k_i = k_c + k_{r,\mathrm{SCM}}(T_i, \varepsilon_i, \varepsilon_{r,i}, d_i, k_{s,i}) \tag{22}$$

in which l_i and l_j are the distance from particle center to the Voronoi face. $k_{r,\mathrm{SCM}}(T_i, \varepsilon_i, \varepsilon_{r,i}, d_i, k_{s,i})$ is the ETC of SCM. The local porosity is

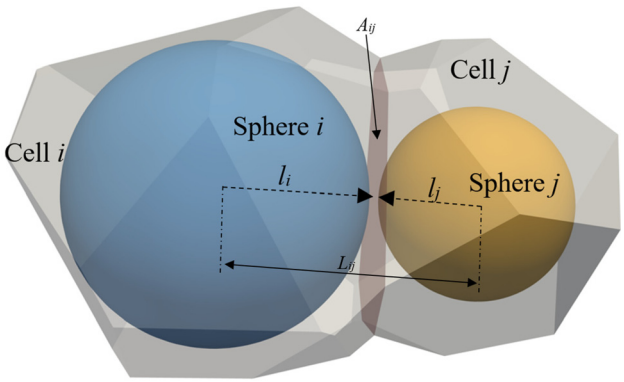

Fig. 6 Voronoi cells of the heat transfer model in nuclear pecked pebble beds

$$\varepsilon_i = 1 - \frac{V_{p,i}}{V_{\text{cell},i}} \tag{23}$$

in which $V_{p,i}$ and $V_{\text{cell},i}$ are the volumes of the particle and the Voronoi cell.

3.2 Model Validation. The packed pebble bed of the TF-PBEC [13,14] is used to validate the particle-scale heat transfer model. TF-PBEC is a part of HTR-PM project [2], and it is conducted by Institute of Nuclear and New Energy Technology (INET) to measure the total ETC under high temperatures. The detail geometrical structure and the packing are shown in Fig. 7. The experimental packed pebble bed is filled with about 70,000 monosized graphite pebbles (60 mm in diameter) without heat source inside. The facility is operated in vacuum condition approximately (<30 Pa), so the heat convection flux is far less than the conduction and radiation, and it is neglected in the simulation.

In the discrete simulation of TF-PBEC, the boundary conditions at top and bottom are adiabatic. The heat flux at inner wall is constant. The temperature of the particles contact with the outer wall is given from the experimental data. The simulation results at 10–140 h are shown in Fig. 8, and the simulation is in good agreement with the experiments. At initial time ($t = 0$ s), all particle temperature and the walls are 22.9 °C. Then the pebbles in the system are heated by the inner wall in the radial direction. The particle temperatures increase gradually and reach the steady-state at 140 h.

3.3 Multicomponent Polydisperse Beds. The discrete heat transfer model is still applicable for the polydisperse beds of multicomponent pebbles. The different packing and Voronoi tessellations of random packing ($\varepsilon = 0.39$) are shown in Fig. 9, the geometry of which is based on the HTTU [12]. At steady-state of packed pebble beds without heat source, the radial ETC k_{eff} can be calculated by

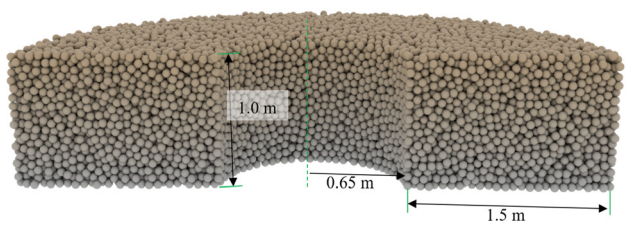

Fig. 7 The structure and packing of the experimental packed pebble bed of the TF-PBEC

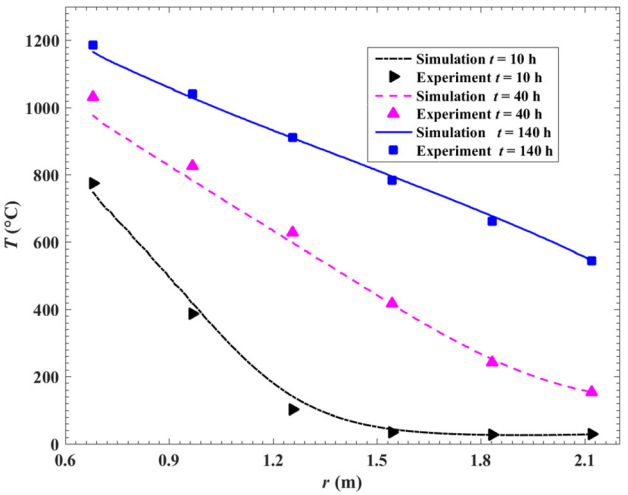

Fig. 8 Experimental results and particle-scale simulation of the transient heat transfer processes of TF-PBEC at half height

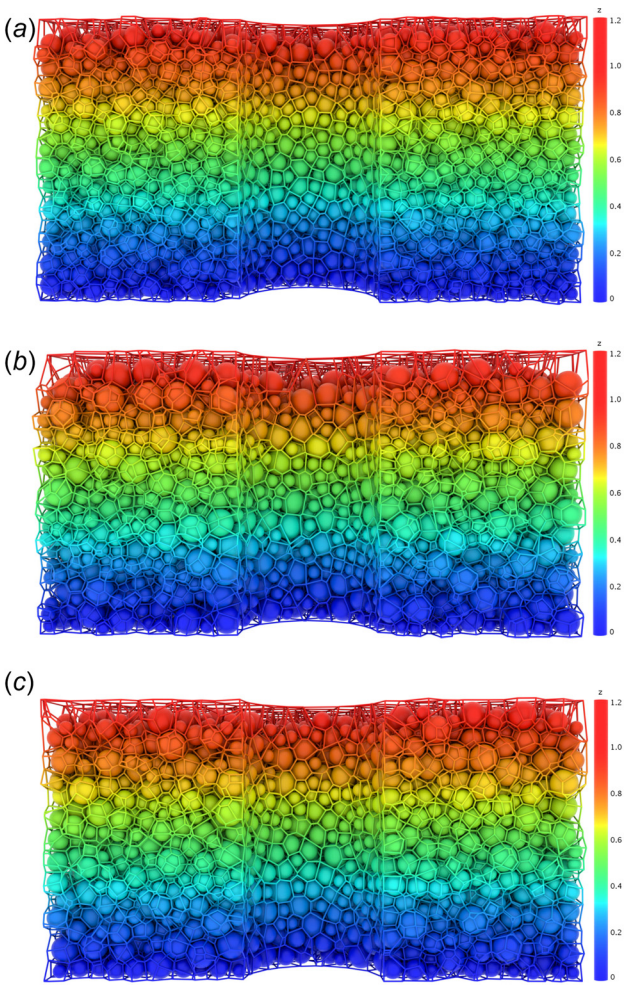

Fig. 9 Packing and Voronoi tessellations of the multicomponent packed pebble beds (x is the volume percentage in all particles): (a) $x_1 = 0.4015$, $d_1 = 60$ mm; $x_2 = 0.5985$, $d_2 = 90$ mm; (b) $x_1 = 0.33$, $d_1 = 60$ mm; $x_2 = 0.67$, $d_2 = 120$ mm; and (c) $x_1 = 0.2104$, $d_1 = 60$ mm; $x_2 = 0.3919$, $d_2 = 90$ mm; $x_3 = 0.3977$, $d_3 = 120$ mm

$$k_{\text{eff}} = \frac{Q}{2\pi L(T_i - T_o)} \ln(r_o/r_i) \tag{24}$$

in which T_i and T_o are the temperatures of inner and outer walls and fixed at given values. Only particle radiation is discussed and

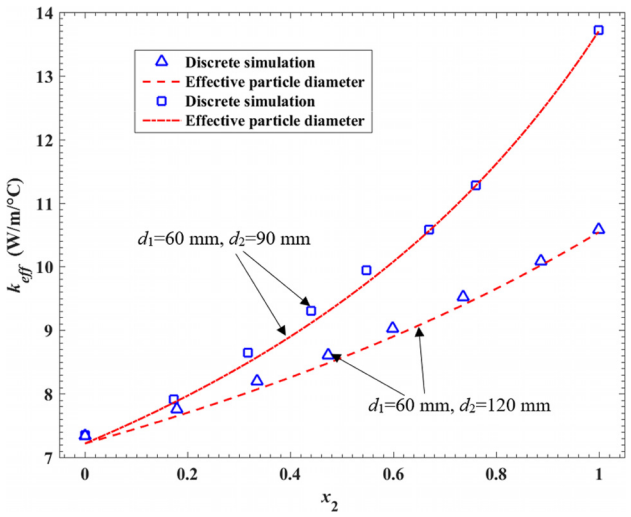

Fig. 10 Discrete simulation and the SCM with effective particle diameter of the binary mixtures of the packed pebble beds at 600 °C

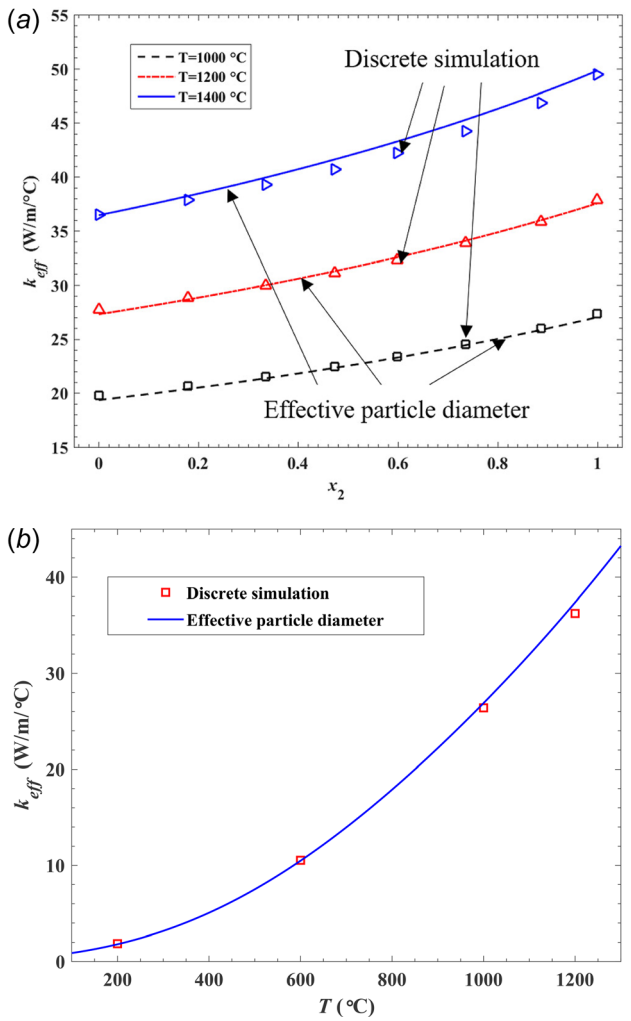

Fig. 11 The ETC of polydisperse packed pebble beds for the binary (*a*) and ternary (*b*) mixtures under different temperatures: (*a*) $d_1 = 60$ mm; $d_2 = 90$ mm and (*b*) $x_1 = 0.2104$, $d_1 = 60$ mm; $_2 = 0.3919$, $d_2 = 90$ mm; $x_3 = 0.3977$, $d_3 = 120$ mm

$k_c = 0$. The total ETC also can be evaluated by SCM. The effective particle diameter of the weighted harmonic mean [10,11] is defined as

$$\frac{1}{d_p} = \sum_{i=1}^{n} \frac{x_i}{d_i} = \frac{x_1}{d_1} + \frac{x_2}{d_2} + \cdots + \frac{x_n}{d_n} \tag{25}$$

where d_i is the particle diameter of the component i and x_i is its volume percentage in all particles.

For the binary mixtures of the packed pebble beds, the average particle temperature in the simulations is 600 °C. For different particle volume percentage of component 2, the results of the discrete simulation and the SCM with effective particle diameter are shown in Fig. 10. When the volume percentage x_2 increases from 0 to 1, the effective particle diameter increases simultaneously and the ETC increases gradually. The predicted values of the SCM with effective particle diameter are in good agreement with the discrete simulations for the binary and ternary mixtures under different temperatures (see Figs. 10 and 11).

4 Conclusions

Particle-scale investigation of the particle thermal radiation is performed for the nuclear packed pebble beds. It is found that:

(1) The SCM is a generic theoretical approach to predict ETC of particle radiation. Based on SCM and radial porosity distribution, the ETC of the radiation decreases significantly at near-wall region.
(2) The particle-scale radiation model is used to discuss the effect of particle surface emissivity. It is shown that radiation exchange factor increases with the surface emissivity. The results of the SCM under different surface emissivity are in good agreement with the existing correlations.
(3) Combined the particle motion and heat transfer model including conduction and radiation, the discrete heat transfer model is presented and it is validated by the transient experimental data.
(4) For the polydisperse beds of multicomponent pebbles, the effective particle diameter in SCM is calculated by weighted harmonic mean of all components. From the simulations under different conditions, the discrete heat transfer model in particle scale is in good agreement with the results of effective particle diameter.

Funding Data

- Foundation for the Author of National Excellent Doctoral Dissertation of the People's Republic of China (Grant No. 201438).
- National Natural Science Foundation of China (Grant Nos. 51406100 and 51576211).
- Science Fund for Creative Research Groups of National Natural Science Foundation of China (Grant No. 51321002).
- China Scholarship Council (CSC) (Grant No. 201506210365).
- National High Technology Research and Development Program of China (863) (Grant No. 2014AA052701).

References

[1] Gao, Z. Y., and Shi, L., 2002, "Thermal Hydraulic Calculation of the HTR-10 for the Initial and Equilibrium Core," Nucl. Eng. Des., **218**(1–3), pp. 51–64.
[2] Zhang, Z. Y., Dong, Y. J., Li, F., Zhang, Z. M., Wang, H. T., Huang, X. J., Li, H., Liu, B., Wu, X. X., Wang, H., Diao, X. Z., Zhang, H. Q., and Wang, J. H., 2016, "The Shandong Shidao Bay 200 MWe High-Temperature Gas-Cooled Reactor Pebble-Bed Module (HTR-PM) Demonstration Power Plant: An Engineering and Technological Innovation," Engineering, **2**(1), pp. 112–118.
[3] Zhang, Z. Y., Wu, Z. X., Wang, D. Z., Xu, Y. H., Sun, Y. L., Li, F., and Dong, Y. J., 2009, "Current Status and Technical Description of Chinese 2 × 250 MWth HTR-PM Demonstration Plant," Nucl. Eng. Des., **239**(7), pp. 1212–1219.
[4] Laubitz, M. J., 1959, "Thermal Conductivity of Powders," Can. J. Phys., **37**(7), pp. 798–808.

[5] Kunii, D., and Smith, J., 1960, "Heat Transfer Characteristics of Porous Rocks," AIChE J., **6**(1), pp. 71–78.
[6] Godbee, H. W., and Ziegler, W. T., 1966, "Thermal Conductivities of MgO, Al_2O_3, and ZrO_2 Powders to 850 °C—Part II: Theoretical," J. Appl. Phys., **37**(1), pp. 56–65.
[7] Botterill, J. S. M., Salway, A. G., and Teoman, Y., 1989, "The Effective Thermal Conductivity of High Temperature Particulate Beds—Part II: Model Predictions and the Implication of the Experimental Values," Int. J. Heat Mass Transfer, **32**(3), pp. 595–609.
[8] Fedina, I., Litovsky, E., Shapiro, M., and Shavit, A., 1997, "Thermal Conductivity of Packed Beds of Refractory Particles: Experimental Results," J. Am. Ceram. Soc., **80**(8), pp. 2100–2108.
[9] Nasr, K., Viskanta, R., and Ramadhyani, S., 1994, "An Experimental Evaluation of the Effective Thermal Conductivities of Packed Beds at High Temperatures," ASME J. Heat Transfer, **116**(4), pp. 829–837.
[10] Gupta, M., Yang, J., and Roy, C., 2002, "Modelling the Effective Thermal Conductivity in Polydispersed Bed Systems: A Unified Approach Using the Linear Packing Theory and Unit Cell Model," Can. J. Chem. Eng., **80**(5), pp. 830–839.
[11] Zbogar, A., Frandsen, F. J., Jensen, P. A., and Glarborg, P., 2005, "Heat Transfer in Ash Deposits: A Modelling Tool-Box," Prog. Energy Combust. Sci., **31**(5–6), pp. 371–421.
[12] Rousseau, P. G., du Toit, C. G., van Antwerpen, W., and van Antwerpen, H. J., 2014, "Separate Effects Tests to Determine the Effective Thermal Conductivity in the PBMR HTTU Test Facility," Nucl. Eng. Des., **271**, pp. 444–458.
[13] Ren, C., Yang, X. T., and Jiang, S. Y., 2016, "Development of Chinese HTR-PM Pebble Bed Equivalent Conductivity Test Facility," ATW. Int. Z. Kernenerg., **61**(1), pp. 23–27.
[14] Ren, C., Yang, X., Jia, H., Jiang, Y., and Xiong, W., 2017, "Theoretical Analysis of Effective Thermal Conductivity for the Chinese HTR-PM Heat Transfer Test Facility," Appl. Sci., **7**(1), p. 76.
[15] Schotte, W., 1960, "Thermal Conductivity of Packed Beds," AIChE J., **6**(1), pp. 63–67.
[16] Wu, H., Gui, N., Yang, X., Tu, J., and Jiang, S., 2016, "Effect of Scale on the Modeling of Radiation Heat Transfer in Packed Pebble Beds," Int. J. Heat Mass Transfer, **101**, pp. 562–569.
[17] Chen, J. C., and Churchill, S. W., 1963, "Radiant Heat Transfer in Packed Beds," AIChE J., **9**(1), pp. 35–41.
[18] Argento, C., and Bouvard, D., 1996, "A Ray Tracing Method for Evaluating the Radiative Heat Transfer in Porous Media," Int. J. Heat Mass Transfer, **39**(15), pp. 3175–3180.
[19] van Antwerpen, W., du Toit, C. G., and Rousseau, P. G., 2010, "A Review of Correlations to Model the Packing Structure and Effective Thermal Conductivity in Packed Beds of Mono-Sized Spherical Particles," Nucl. Eng. Des., **240**(7), pp. 1803–1818.
[20] Rycroft, C. H., Grest, G. S., Landry, J. W., and Bazant, M. Z., 2006, "Analysis of Granular Flow in a Pebble-Bed Nuclear Reactor," Phys. Rev. E, **74**(2), p. 021306.
[21] Wu, H., Gui, N., Yang, X., Tu, J., and Jiang, S., 2016, "Effects of Particle Size and Region Width on the Mixing and Dispersion of Pebbles in Two-Region Pebble Bed," Granular Matter, **18**(4), p. 76.
[22] Wu, H., Gui, N., Yang, X., Tu, J., and Jiang, S., 2017, "Numerical Simulation of Heat Transfer in Packed Pebble Beds: CFD-DEM Coupled With Particle Thermal Radiation," Int. J. Heat Mass Transfer, **110**, pp. 393–405.
[23] Wu, H., Gui, N., Yang, X., Tu, J., and Jiang, S., 2018, "A Smoothed Void Fraction Method for CFD-DEM Simulation of Packed Pebble Beds With Particle Thermal Radiation," Int. J. Heat Mass Transfer, **118**, pp. 275–288.
[24] Wu, H., Gui, N., Yang, X., Tu, J., and Jiang, S., 2017, "Modeling Effective Thermal Conductivity of Thermal Radiation for Nuclear Packed Pebble Beds," ASME. J. Heat Transfer, **140**(4), p. 042701.
[25] De Beer, M., Du Toit, C. G., and Rousseau, P. G., 2017, "A Methodology to Investigate the Contribution of Conduction and Radiation Heat Transfer to the Effective Thermal Conductivity of Packed Graphite Pebble Beds, Including the Wall Effect," Nucl. Eng. Des., **314**, pp. 67–81.
[26] Talukdar, P., and Mishra, S. C., 2003, "Transient Conduction-Radiation Interaction in a Planar Packed Bed With Variable Porosity," Numer. Heat Transfer, Part A, **44**(3), pp. 281–297.
[27] Wu, J. W., and Chu, H. S., 1999, "Combined Conduction and Radiation Heat Transfer in Plane-Parallel Packed Beds With Variable Porosity," J. Quant. Spectrosc. Radiat. Transfer, **61**(4), pp. 443–452.
[28] Methnani, M., and Tyobeka, B., 2013, *Evaluation of High Temperature Gas Cooled Reactor Performance: Benchmark Analysis Related to the PBMR-400, PBMM, GT-MHR, HTR-10 and the ASTRA Critical Facility*, International Atomic Energy Agency, Vienna, Austria.
[29] Bahrami, M., Yovanovich, M. M., and Culham, J. R., 2006, "Effective Thermal Conductivity of Rough Spherical Packed Beds," Int. J. Heat Mass Transfer, **49**(19–20), pp. 3691–3701.
[30] van Antwerpen, W., Rousseau, P. G., and du Toit, C. G., 2012, "Multi-Sphere Unit Cell Model to Calculate the Effective Thermal Conductivity in Packed Pebble Beds of Mono-Sized Spheres," Nucl. Eng. Des., **247**, pp. 183–201.
[31] White, S. M., and Tien, C. L., 1987, "Analysis of Flow Channeling Near the Wall in Packed-Beds," Warme Stoffubertrag, **21**(5), pp. 291–296.
[32] Amiri, A., and Vafai, K., 1994, "Analysis of Dispersion Effects and Non-Thermal Equilibrium, Non-Darcian, Variable Porosity Incompressible Flow Through Porous Media," Int. J. Heat Mass Transfer, **37**(6), pp. 939–954.
[33] Vafai, K., 1984, "Convective Flow and Heat Transfer in Variable-Porosity Media," J. Fluid Mech., **147**(1), pp. 233–259.
[34] Du Toit, C. G., 2008, "Radial Variation in Porosity in Annular Packed Beds," Nucl. Eng. Des., **238**(11), pp. 3073–3079.
[35] Kaviany, M., 1991, *Principles of Heat Transfer in Porous Media*, Springer-Verlag, New York.
[36] Hunt, M. L., and Tien, C. L., 1990, "Non-Darcian Flow, Heat and Mass-Transfer in Catalytic Packed-Bed Reactors," Chem. Eng. Sci., **45**(1), pp. 55–63.
[37] Benenati, R. F., and Brosilow, C. B., 1962, "Void Fraction Distribution in Beds of Spheres," AIChE J., **8**(3), pp. 359–361.
[38] Mueller, G. E., 1992, "Radial Void Fraction Distributions in Randomly Packed Fixed Beds of Uniformly Sized Spheres in Cylindrical Containers," Powder Technol., **72**(3), pp. 269–275.
[39] De Klerk, A., 2003, "Voidage Variation in Packed Beds at Small Column to Particle Diameter Ratio," AIChE J., **49**(8), pp. 2022–2029.
[40] Theuerkauf, J., Witt, P., and Schwesig, D., 2006, "Analysis of Particle Porosity Distribution in Fixed Beds Using the Discrete Element Method," Powder Technol., **165**(2), pp. 92–99.
[41] Howell, J. R., Menguc, M. P., and Siegel, R., 2010, *Thermal Radiation Heat Transfer*, CRC Press, Boca Raton, FL.
[42] Wen, C. D., and Mudawar, I., 2006, "Modeling the Effects of Surface Roughness on the Emissivity of Aluminum Alloys," Int. J. Heat Mass Transfer, **49**(23–24), pp. 4279–4289.
[43] King, J., Jo, H., Tirawat, R., Blomstrand, K., and Sridharan, K., 2017, "Effects of Surface Roughness, Oxidation, and Temperature on the Emissivity of Reactor Pressure Vessel Alloys," Nucl. Technol., **200**(1), pp. 1–14.
[44] Argo, W. B., and Smith, J. M., 1953, "Heat Transfer in Packed Beds," Chem. Eng. Prog., **49**(8), pp. 443–451.
[45] Wakao, N., and Kato, K., 1969, "Effective Thermal Conductivity of Packed Beds," J. Chem. Eng. Jpn., **2**(1), pp. 24–33.
[46] Ai, J., Chen, J. F., Rotter, J. M., and Ooi, J. Y., 2011, "Assessment of Rolling Resistance Models in Discrete Element Simulations," Powder Technol., **206**(3), pp. 269–282.
[47] Thornton, C., Cummins, S. J., and Cleary, P. W., 2013, "An Investigation of the Comparative Behaviour of Alternative Contact Force Models During Inelastic Collisions," Powder Technol., **233**, pp. 30–46.